Received: February 26, 2024. Revised: April 28, 2024.

International Journal of
Intelligent Engineering & Systems

http://www.inass.org/

Adaptive Gamma and Color Correction for Enhancing Low-Light Images

Ali Hakem Alsaeedi[1,2]* **Suha Mohammed Hadi[1]** **Yarub Alazzawi[3]**

[1]*Informatics Institute for Postgraduate Studies, Iraqi Commission for Computer and Informatics, Bagdad, Iraq*
[2]*College of Computer Science and Information Technology, University of Al-Qadisiyah, Al Diwaniyah, Iraq*
[3]*Al-Khwarizmi College of Engineering, University of Baghdad, Baghdad, Iraq*
* Corresponding author's Email: phd202130687@iips.edu.iq

Abstract: Low-light images have faded color, low color rates, and unclear image details. It significantly affects the performance of computer vision applications. Low-light image processing systems increase the color rate to restore the original image, and the color balance must be maintained for the image to be of high quality. In this paper, adaptive gamma and color correction (AGCC) is proposed as a method to enhance low-light images. The proposed model aims to enhance the color rates and balance of images to restore the original color in the image. It consists of three basic steps: calculate the adaptive gamma suitable for the lighting in the image, correct color, and starch color intensity over the histogram. Eight datasets containing images with diverse lighting conditions were employed to evaluate the proposed model's performance. The experimental results show that the proposed model archives outperform the state-of-the-art regarding computational simplicity, time complexity, and enhancement efficiency of the restored images. The model significantly improves processing time, retrieving images in an average of 0.09 Sec. from the evaluated datasets. Furthermore, it demonstrates a performance advantage exceeding 85% compared to methods in state-of-the-art.

Keywords: Low-light image enhancement, Atmospheric scattering model, Adaptive gamma correction, Color normalization.

1. Introduction

Image enhancement occupies a significant field in improving the performance of digital devices that depend on computer vision, such as auto driving [1], [2], pattern recognition [3], face recognition [4], and other applications. Technically, the quality of the image depends on the accuracy of the image details and characteristics in terms of normal illuminance, contrast, and color distribution. As long as the color density distribution is closer to the normal distribution, it produces an image with clear details [5]. Fig. 1 shows a distributed intensity color of images in low, normal, and high light conditions.

Images are affected by several factors; one of the most important factors is an atmospheric effect, such as fog, haze, dust, sand, low and high lighting. It directly affects the balance of color, increasing the density of one color over the rest of the color channels R, G, and B) depending on the channel wavelet, absorption by weather particles, and light conditions.

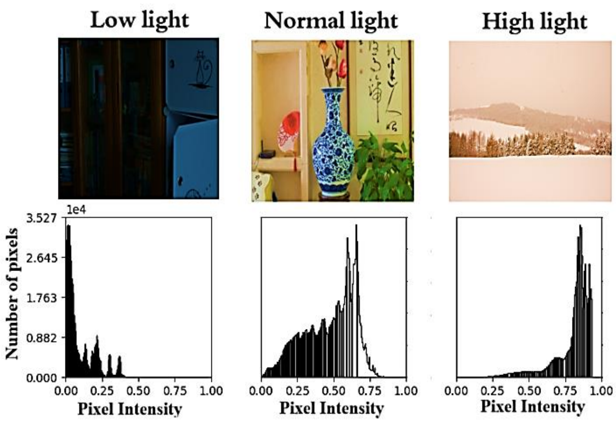

Figure. 1 Low, normal, and high light image with intensity color distribution

Regards to average channels R, G, and B, low-light always have low rates always have low rates.

Improving these images increases color rates while maintaining a balance between rates so that the image is high quality without vail. Images lose most of their details when taken in low lighting because most information and image details are apparent in normal light. The challenges facing the processing of low-light images are that the image is either completely dark or partially dark; that is, part of the image has high light, and part of the image has low light. Therefore, dynamic contrast plays an important role in improving lighting by balancing the color in the image.

There are three approaches for low-light image enhancement (LIE) machine learning, Retinex theory, and atmospheric scattering model (ASM)[6]. Technically, the model based ASM depends on the nature of the pixel and has less complicated than the other models because the model based ASM methods don't require extensive training on large datasets[7]. Therefore, it is faster and more suitable for real-time applications on diverse lighting images.

The LIE models usually consist of several steps to restore natural lighting in the image, and the general operation of these steps can be described as lighting improvement color and contrast correction[6, 8, 9]. The gamma correction plays an effective role in improving lighting in the image in LIE models[6]. The value of gamma is directly proportional to the amount of lighting, so the higher the value of gamma, the more the purity of the image increases, and the less it decreases the purity of the image. The value of gamma should be appropriate for the image, so we relied in this research on calculating the value of gamma to be appropriate for the nature of the image and the lighting details in the image.

We focus in this model on achieving the following contributions:

1. Reducing the computational complexities in the proposed model increases the processing speed and reduces space complexities.
2. Restoring the image with a high accuracy color distributed with normal lighting that is very similar to the natural image.
3. Choosing the basic parameters, such as the appropriate gamma value for the lighting in the image and processing images with mixed lighting.

The rest of the paper is organized into 6 sections as follows: section 2: related works, section 3: atmospheric scattering model, section 4: effect gamma correction and the image luminous, section 5: proposed model, section 6: results discussion, and finally, section 7: conclusion.

2. Related works

There are multiple challenges in improving image lighting quality. Some of these challenges are adding unwanted colors to the enhanced image(artifact), appearing hale around objects, the lighting not ultimately reaching the desired quality (either high or low), and a high amount of noise. That makes the improvement efforts fall short of achieving the intended aim. There are many enhancing for light images in different approaches of LIE.

Gang et al. [10] proposed a method for contrast enhancement of brightness-distorted images using an improved adaptive gamma correction technique. This method involves classifying images into two categories—dim and bright—based on a comparison of the average intensity level of the Y channel (from the YCrCb color space) with a predetermined threshold. This classification enables the application of tailored image enhancement strategies that cater to the specific needs of each image type, thereby improving contrast and visibility. For dimmed images, they employed a gamma correction modulated by a truncated Cumulative Distribution Function (CDF) for enhancement. Conversely, for bright images, they used negative images in conjunction with a CDF for enhancement. By dividing the images according to a certain threshold, the model may fail to enhance images with different lighting in the same image; therefore, the resulting image is of low quality.

in [11] Shijie et al. proposed a low light image enhancement technique based on Retinex theory. The authors introduce a semi-decoupled Retinex image decomposition method, leveraging a Gaussian Total Variation model for gradual illumination estimation directly from the input image and a joint estimation of the reflectance layer using both the input and intermediate illumination layers. This technique concurrently reduces imaging noise while estimating the reflectance layer. The complexities used in this work increase the time complexity in implementation, which reduces the algorithm's efficiency, and the resulting images were not very efficient.

Jong et al. [6] proposed an atmospheric scattering model for enhancing low-light images using gamma correction before mixed color spaces. The authors propose a transmission map derived as a function of two saturations of the original image in two color spaces1. Due to the difficulty in estimating the saturation of the original image, the transmission map is converted into a function of the average and maximum values of the original image. These two values are estimated from a given low-light image using the gamma correction prior. In addition, a pixel-adaptive gamma value determination algorithm is proposed to prevent under- or over-enhancement. The limitation of this proposed model is that there are too many complications with using more than one color space -there are many conversions between color spaces-. However, the model did not recover images with high opacity and high efficiency, so the images were recovered with a lot of noise in the image, which reduced the quality of the recovered images.

In the study [12], the authors proposed a method for enhancing images captured in low-light conditions. The method begins by inverting a low-light image to obtain a foggy image. This inversion is a uniform and reversible operation performed on the entire image. The inverted image is then used as the input and passed through the atmospheric light and transmission estimation modules. In one part of the system, the authors use a Gaussian Filter, which blurs the edges of the resulting images, thereby reducing their sharpness. Despite the use of the filter to reduce the noise present in the image, images captured in low light conditions were not of high clarity. This is because severe noise dominates the retrieved image. After applying the Gaussian Filter, the image becomes utterly blurred due to the filter's effect, which increases the blurring of the image in an attempt to reduce the high noise.

The authors in the study [13] proposed a Retinex base model to enhance low-light images by unveiling their underlying structure through robust Retinex models. This approach focuses on separating an image's illumination and reflectance components to adjust the lighting, improving image visibility and color fidelity. The limitation of this model is that the method is usually complicated and requires time complications. In addition, the restored images fade and are low quality.

3. Atmospheric scattering model (ASM)

The ASM model describes how light is scattered by the atmosphere before it reaches the camera[14]. At the same time, the models attempt to estimate the transmission map of pixels over different atmospheric effects, such as haze, low light, and dust sand. The image in the ASM typically be affected directly by transmission and atmospheric light, as shown in Eq. (1)[15]:

$$I_{x,y} = T_{x,y} \cdot L_{x,y} + A(1 - T_{x,y}) \tag{1}$$

Where: $I_{x,y}$ is the observed intensity, $T_{x,y}$ is the transmission, $L_{x,y}$ is the scene radiance, and A is the atmospheric light.

The value of the transmission map ($T_{x,y}$) within the interval [0, 1], where 0 means the atmosphere has a high effect on the scene (worst situation) and in 1 the camera capturing the scene in an ideal situation. Therefore, most image enhancement techniques focus on mitigating the effects of atmospheric conditions to improve the transmission map, thereby achieving higher image quality. This is accomplished through various methods such as Gamma correction (GC)[16], the Dark Channel Prior principle (DCP)[17], Histogram Equalization (HE)[9], or any approach that contributes to enhancing color contrast and color density in the image. These techniques assist in removing haze, dust, or sand effects that impact image clarity and adjust lighting and colors to appear closer to reality as if captured under ideal lighting conditions.

When using gamma correction with a model based on ASM to adjust image brightness to match viewing conditions, enhance visual quality by fine-tuning brightness and contrast[18]. The process ensures images are rendered with luminance that aligns with human perception across different lighting environments. This emphasizes the importance of gamma correction in digital imaging. Color correction entails adjusting colors in an image to reflect how they would appear accurately under ideal lighting conditions[19]. The GC includes modifying the saturation, hue, and color balance of lights and shadows within the image. Combining gamma adjustment to increase illumination with color correction to maintain natural colors can significantly improve low-light images, resulting in more attractive and realistic final images. Integrating gamma and color correction techniques is crucial in digital imaging, particularly when poor lighting conditions [20]. The dual approach enhances visibility in dimly lit images and preserves color fidelity, ensuring images remain true to their original appearance. Advanced image processing tools and software offer sophisticated options for fine-tuning both aspects, enabling photographers and image editors to achieve the desired balance between light and color[21]. The balance is essential for producing high-quality images that convey the intended message or emotion while accurately representing visual reality[5].

4. Effect GC on image brightness:

The GC is a nonlinear operation used in image processing to adjust the luminance of an image [22]. The primary purpose of GC in image processing is to enhance the low-light image. Eq. (2) shows the basic form of GC[15].

Received: February 26, 2024. Revised: April 28, 2024.

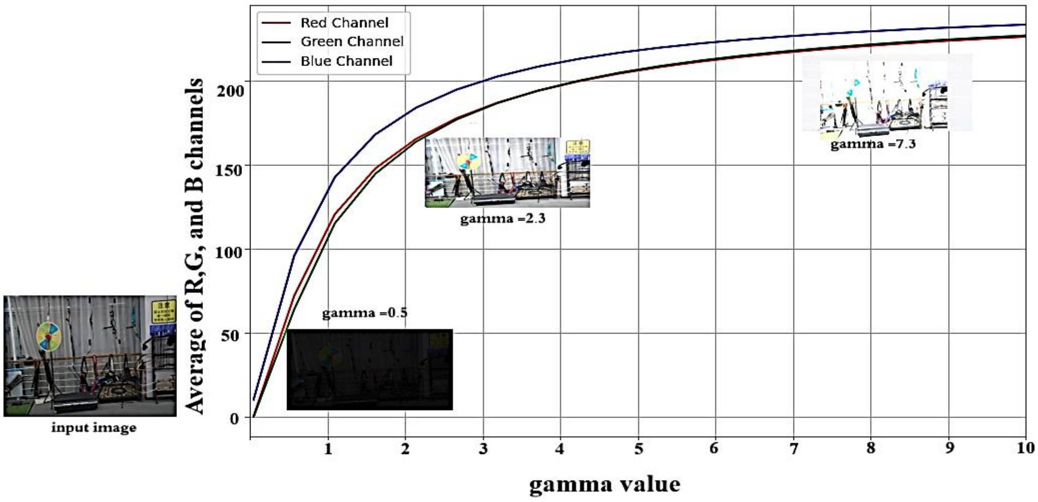

Figure. 2 Effect gamma value on brightness and average R, G, and B channel

$$I'_x = A \times (I_x)^{\gamma} \tag{2}$$

Where: I'_x is the output image value, is the input image, γ is the gamma value, a constant that defines the nonlinearity of the encoding or decoding process, is a scaling constant, often set to 1 for simplicity in many applications. Most image processing processes prefer to normalize the value of pixels between [0, 1] to avoid information loss induced by overflow truncation[23]. Using fixed gamma values for image enhancement can lead to either too much or too small adjustment, as images taken in low-light conditions come from a wide range of lighting situations. To overcome this issue, the adaptive value of gamma values is based on the local brightness of the image, which is necessary when applying GC. That means that areas of the image that are already well-lit will be treated with a smaller gamma value to avoid over-brightening. in comparison, the darker areas will receive a larger gamma value to increase visibility. Fig. 2 illustrates the effect of different gamma (γ) on the image brightness and the average value of R, G, and B channels.

Color intensity is concentrated in the first quarter of the histogram for images with low light. That indicates a predominance of darker tones that make image details challenging to distinguish, negatively affecting image quality. Conversely, in brightly lit images, color intensity is more evident in the first half of the histogram. The points to a concentration in lighter shades, which may result in less detail in the brighter areas[24]. The images that highlight the color intensity gather in the last quarter of the histogram, leading to faded color and reducing contrast and vibrancy. Natural-looking images, however, display an even color distribution across the histogram, reflecting a balance of light and shadows that usually translates to better image quality[25].

The balanced distribution helps maintain details and contrast, making the image appear more natural and appealing. Hence, image processing applications strive to optimize color distribution to maintain balance and prevent excessive concentration of any single channel[26]. That could detract from the overall image quality. The goal is to achieve optimal contrast and even color distribution to enhance the beauty and realism of the image, making it more attractive and life-like.

5. Proposed AGCC model

The objectives of the proposed model are:

1. Reducing the amount of noise in the final image better than the existing smoothing filters.
2. Maintain the original color and avoid artificial colors not present in the original scene.
3. To address images with varied lighting within the same scene and prevent overexposure in the final output, employing an adaptive model and local tone mapping is essential for balancing illumination and preserving natural scene details.

The proposed method consists of three steps as follows.

step1. Adaptive gamma correlation.
step2. Color correction based on the mean value of high channel (R,G, and B).
step3. Contrast color normalization.

5.1 Proposed AGCC model

The value AGC depends on two factors luminance and the average of three color channels R, G, and B.

Received: February 26, 2024. Revised: April 28, 2024.

Table 1. shows the scenarios that are expected with the value of γ in adaptive GC.

Type of image	L	Ĭ	γ
dim	low	low	≤2
optimal	0.5	1	1
bright	high	high	≥2

- **Luminance factor (L):** luminance in images expresses the image's brightness level. Eq. (3) calculates luminance(L) of image [25]:

$$L = 0.2126 I_R^c + 0.7152 I_G^c + 0.0722 I_B^c \tag{3}$$

Where: I_R^c , I_G^c, and I_B^c are the mean of red, green, and blue channels respectively.

- **Average colors factor ($\breve{I}$):** The average colors factor is the sum of the average three colors (I_R , I_G, and I_B). Eq. (4) calculates the average color factor:

$$\breve{I} = \frac{\sum_{i=1}^{n} I_i^c}{3} \tag{4}$$

Where c is 1,2,3, I_i^c average of channels R, G, B. To calculate the optimal value of gamma, we depend on the content of nature (global image) in term average colours (1) and optimal luminance (0.5). Eq. (5) calculates the adaptive gamma correction:

$$\gamma = \gamma_c + [(0.5 - L) \times (1 - \breve{I})] - 2L \tag{5}$$

Where: γ_c is the control parameter of γ. In the proposed model the γ_c is 2.0. Eq. (2) is modified to be suitable to the new gamma (γ) that is obtained from Eqs. (5). and (6) presents the new formal GC.

$$I'_x = A \times (I_x)^{1/\gamma} \tag{6}$$

Table 1 shows the scenarios that are expected with the value of γ in adaptive GC.

The color correction step calibrates the colors in image by adjusting the intensity levels of each color channel. In this step, the proposed model achieves a uniform average value of the R, G, and B channels. The function adjusts the intensity values for each color channel by adding a scaled difference between the mean intensity of that channel. Eq. (7) represents the adjusted intensity for the color channel in the image.

$$I'_i(x,y) = I_i(x,y) + (I_{max}^c - I_i^c) I_i(x,y \tag{7}$$

Where: $I_i(x,y)$ is value of a pixel in the location (x,y) of the input image, $I_i^{'}(x,y)$ output value, and I_{max}^c the maximum mean of the three color channels.

5.2 Color correction

The AGC (step 1) enhances the image overall without focusing on the image's details. Therefore, it is necessary to refine the image's details. The contrast stretching process aims to make these details more visible by increasing the intensity difference between the lighter and darker parts of the image. This process adjusts each pixel's intensity in the image from the original range to the target range. It identifies the minimum and maximum intensity values present in the original image. Alternatively, more sophisticated approaches determine specific low and high percentile values (e.g., 2nd and 98th percentiles) to exclude outliers. Eq. (8) calculates the Contrast color enhancement.

$$I' = \frac{(I - I_{\min}) \times (O_{\max} - O_{\min})}{(I_{\max} - I_{\min})} + O_{\min} \tag{8}$$

where: I' is the new intensity value of the pixel. I is the original intensity value of the pixel. $I_{\min}$ and $I_{\max}$ are the minimum and maximum intensity values in the original image, respectively. $O_{\min}$ and $O_{\max}$ are the minimum and maximum intensity values in the target range, respectively. These parameters define the target range of intensity values, which often corresponds to the maximum range supported by the image format or display device. For an 8-bit grayscale image, this range is typically 0 to 255

The overall algorithm of the proposed AGCC model is presented in algorithm I.

Algorithm I: AGCC model

Input: low light image (I)
Output: Enhanced image (I')
Applied the AGC on the input image (I) (Eq.6)
Applied the color correction on the result of step 1 (Eq. 7)
Applied the contrast color enhancement on the result of step 2. (Eq.8)
Return Enhanced image (I')

Fig. 3 shows the result of each step of the proposed AGCC model with histogram, average (I), and standard division (std) of each R, G, and B channel.

Fig. 4 shows the result of the applied proposed AGCC model on different samples of low light images. As shown in Fig. 4, the restored lowlight

Received: February 26, 2024. Revised: April 28, 2024.

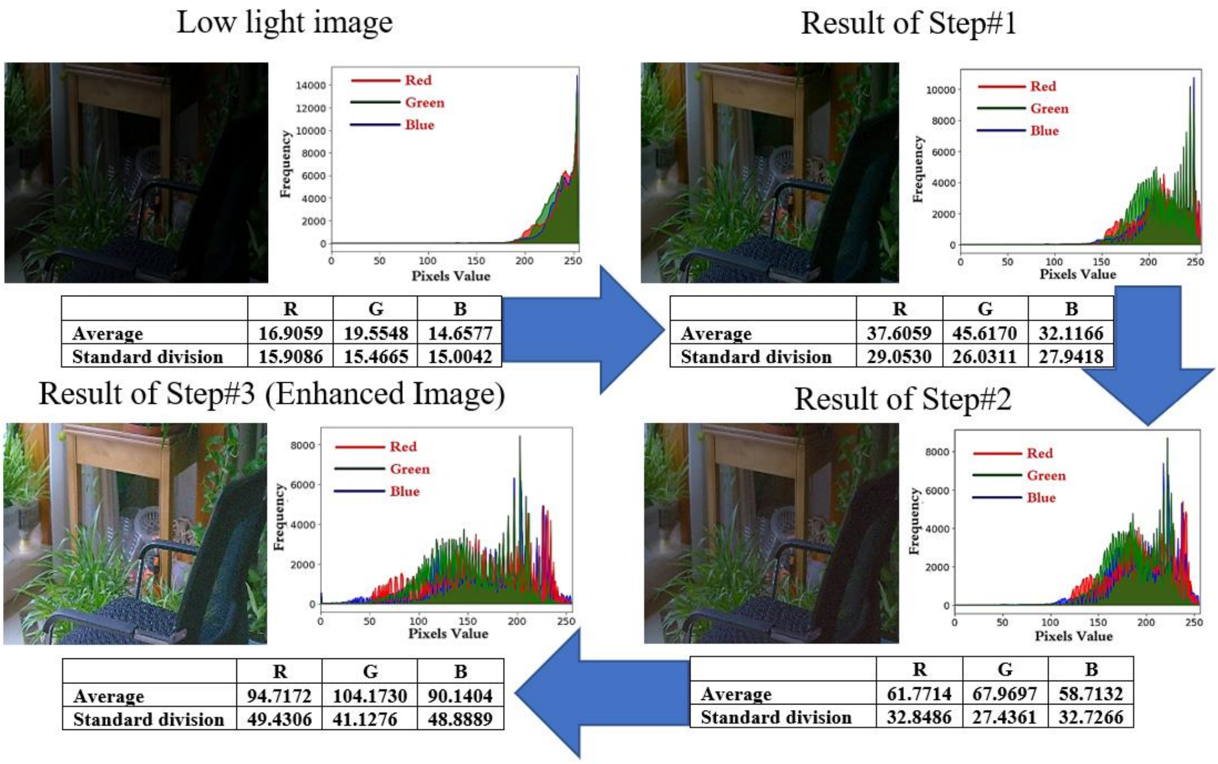

	R	G	B
Average	16.9059	19.5548	14.6577
Standard division	15.9086	15.4665	15.0042

	R	G	B
Average	37.6059	45.6170	32.1166
Standard division	29.0530	26.0311	27.9418

	R	G	B
Average	61.7714	67.9697	58.7132
Standard division	32.8486	27.4361	32.7266

	R	G	B
Average	94.7172	104.1730	90.1404
Standard division	49.4306	41.1276	48.8889

Figure. 3 A three-step process of proposed AGCC model illustrated by average , standard deviation R, G, and B Channels and Histograms

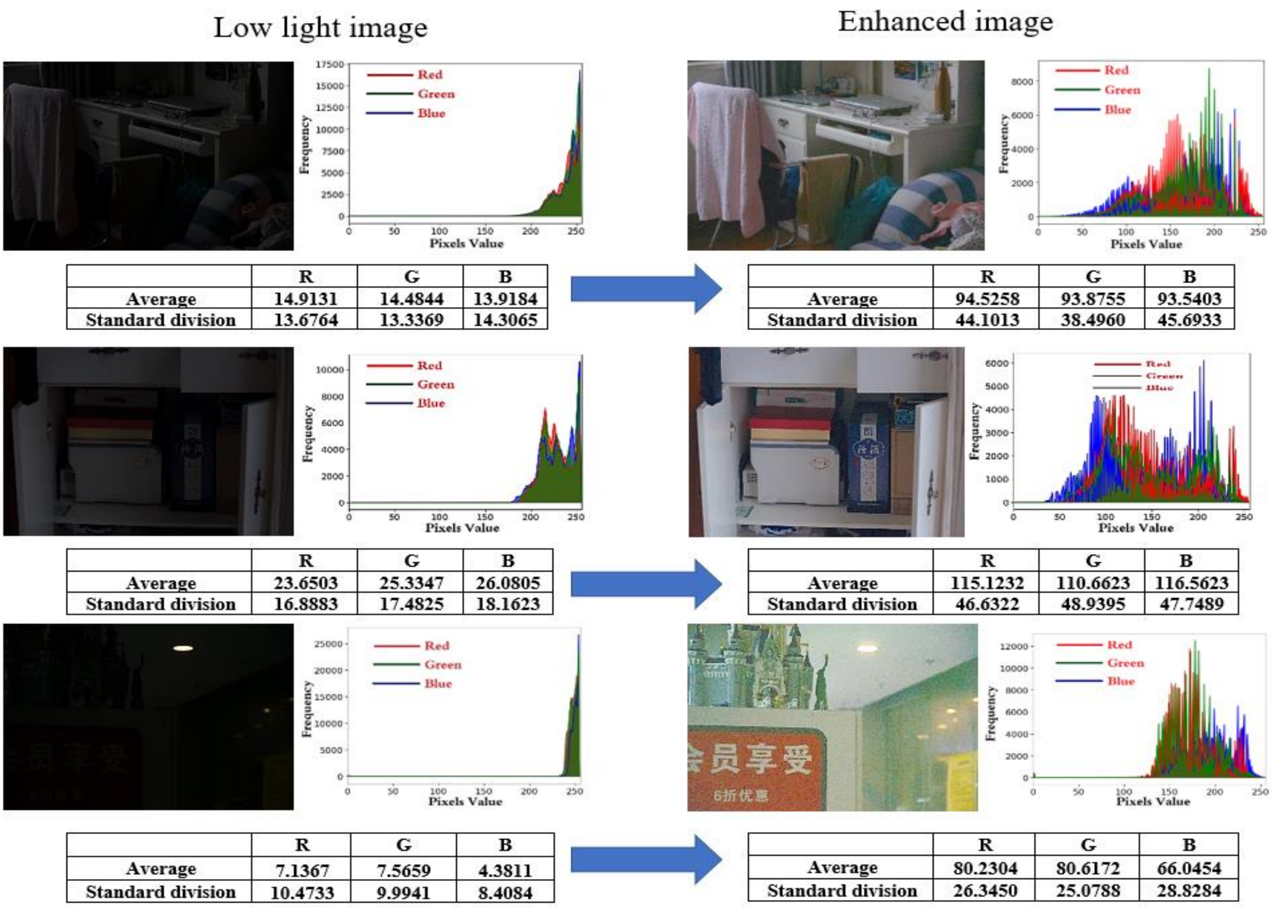

	R	G	B
Average	14.9131	14.4844	13.9184
Standard division	13.6764	13.3369	14.3065

	R	G	B
Average	94.5258	93.8755	93.5403
Standard division	44.1013	38.4960	45.6933

	R	G	B
Average	23.6503	25.3347	26.0805
Standard division	16.8883	17.4825	18.1623

	R	G	B
Average	115.1232	110.6623	116.5623
Standard division	46.6322	48.9395	47.7489

	R	G	B
Average	7.1367	7.5659	4.3811
Standard division	10.4733	9.9941	8.4084

	R	G	B
Average	80.2304	80.6172	66.0454
Standard division	26.3450	25.0788	28.8284

Figure. 4 Lowlight image and their restoration by proposed AGCC model

images obtained by using the proposed model have a nearly simultaneous histogram. Moreover, The average of red, blue, and green is approximately equal. Even if there was a difference in the color values of the three basic colors, the difference was not significant.

6. Result discussion

To evaluate the performance of the proposed AGCC was tested on two datasets. The result of the proposed model compares the result with five of the state-of-the-art algorithms: IAGC [10], LGMS [11], LIEW [6], REN [13], and LLEI [12].

6.1 Dataset description

Six low light datasets are used in test the validity of the proposed model. It is grouped in two categories full reference datasets, and nan-reference datasets

1. **Full reference dataset** is a dataset that has ground truth used in image quality assessment. In this paper used two datasets of full reference datasets LOL and GladNet. LOL is located in [27]. The LOL dataset consists of 485 pairs (full reference) of images. The GladNet is located in [28], it a content of 5000 low -light images.
2. **Nan reference dataset** is a dataset that does note has ground truth used in image quality assessment. In this paper used four datasets of nan reference datasets Zero_test, DICM, LIME, and VV. Zero_test is 64 images have high darkness taken from test data in[23]. The DICM in [30] consists of 44 lowlight images. The LIME is located in [29] which has 69 low light images. The final dataset is VV from [31] containing 10 images.

6.2 Computation time

The proposed method was implemented on a 12th Gen Intel® Core™ i9 -12900H CPU running at 2.90 GHz with 16 GB RAM without multithreading acceleration. We used the same code and platform as described in the paper's project. All algorithms were executed on the same computer. The image reading and saving process was exclusive. Table 2 shows the execution time and platform used by competitive algorithms. The proposed method achieved a fast execution time for all images compared with models in the state -of -the -art. The IAGC [10] had the second -fastest execution time, and its overall average execution time was about 44% slower than that of the proposed AGCC model. The REN [13] has high computational costs and is slower compared with the state -of -the -art models.

6.3 Quantitative comparison

To examine the quantitative of restore images used metrics based in availability of ground truth. The full reference dataset used to assess image metrics measured the similarity between restored images and ground truth. These metrics are the Structural Similarity Index Measure (SSIM), and Peak Signal -to -Noise Ratio (PSNR).

The nan - refences datasets used to evaluate image quality assessment (NR -IQA) metrics are the natural Image Quality Evaluator (NIQE), Blind/Reference less Image Spatial Quality Evaluator (BRISQUE). The NIQE measures the accurate features extracted from the restored image. BRISQUE measures the correct color distribution and measures how it close to normal distribution.

Tables 3 and 4 show the results of the proposed model and comparison algorithms on full reference datasets in terms of PSNR and SSIM, respectively. From the Table 3, we observe that the proposed AGCC model achieved the best results in terms of PSNR followed by the LLEI [12] and LGMS [11] method. The proposed system's superiority attributed to its reliance on restoring the original colors by

Table 2. Comparison of Average Execution Time of Proposed AGCC Model vs. State -of -the -Art Models

Algorithm	**Time (Sec) per image of each dataset**						**Simulation language**
	LOL	Zero_test	GladNet	DICM	VV	LIME	
IAGC[10]	0.102	0.100	0.147	0.161	0.129	0.193	Python
LGMS[11]	0.108	0.113	0.18	0.180	0.212	0.203	Python
LLEI[12]	0.124	0.109	0.153	0.170	0.201	0.221	Python
LIEW[6]	0.325	0.481	0.289	0.406	0.327	0.398	MATLAB
REN[13]	0.530	0.481	0.449	0.465	0.481	0.438	MATLAB
Proposed AGCC	0.051	0.063	0.096	0.124	0.098	0.109	Python

Table 3. Comparison of result of the proposed AGCC Model vs. State -of -the -Art Models in terms of PSNR↑

Algorithm	**Dataset**	
	LOL	**GladNet**
IAGC[10]	11.250	16.127
LGMS[11]	15.830	17.122
LLEI[12]	15.498	17.941
LIEW[6]	12.470	18.808
REN[13]	9.902	14.278
Proposed AGCC	17.269	19.476

Table 4. Comparison of result of the proposed AGCC Model vs. State -of -the -Art Models in terms of SSIM↑

Algorithm	**Dataset**	
	LOL	**GladNet**
IAGC[10]	0.469	0.772
LGMS[11]	0.475	0.821
LLEI[12]	0.464	0.701
LIEW[6]	0.639	0.717
REN[13]	0.410	0.546
Proposed AGCC	0.710	0.870

leveraging the quality metrics and attempting to approximate the modified colors to the ideal colors in the image. By applying equations that bring the colors closer to the ideal colors in the image, the model achieved results close to the ground truth images compared to the proposed algorithms

Table 4 shows that the proposed model shows superior performance with a similarity rate regraded to SSIM metrics of up to 0.87 in the GladNet and 0.71 in the LOL database, which corresponds to an average SSIM of about 0.7 with the original images in ground truth. On the other hand, the second ranked model, the LGMS[11] model, achieved good results but lower compared to the proposed model, while the REN[13] algorithm showed lower performance as it relied on retinex techniques that affect the similarity between the retrieved images and ground truth.

If we take the average of the two databases concerning Tables 3 and 4, we find that the gamma correction -based models (IAGCC [10] and

Table 5. Comparison of result of Proposed AGCC Model vs. State -of -the -Art Models in terms of NIQE↓ on Nan reference datasets

Algorithm	**Dataset**					
	Zero_test	**VV**	LIME	DICM	HED -BSDS	UCID_V2
IAGC[10]	5.412	2.923	3.948	4.007	3.154	3.543
LGMS[11]	6.960	2.966	4.385	3.936	3.660	3.652
LLEI[12]	5.962	2.499	3.994	3.320	3.104	3.653
LIEW[6]	5.840	2.591	4.086	3.513	3.431	3.734
REN[13]	7.032	3.973	5.257	6.100	4.287	5.235
Proposed AGCC	5.398	2.698	3.680	3.216	3.041	3.539

Table 6. Comparison of result of Proposed AGCC Model vs. State -of -the -Art Models in terms of BRSQUE↓ on Nan reference datasets

Algorithm	**Dataset**					
	Zero_test	**VV**	LIME	DICM	HED -BSDS	UCID_V2
IAGC[10]	36.296	16.769	17.168	22.429	10.027	17.946
LGMS[11]	49.688	19.165	24.743	30.716	18.091	24.730
LLEI[12]	38.067	20.975	18.736	20.850	12.018	18.341
LIEW[6]	39.502	20.475	18.868	20.815	12.911	18.603
REN[13]	50.814	32.592	26.445	38.416	20.349	27.548
Proposed AGCC	35.691	17.961	14.679	20.010	9.546	16.450

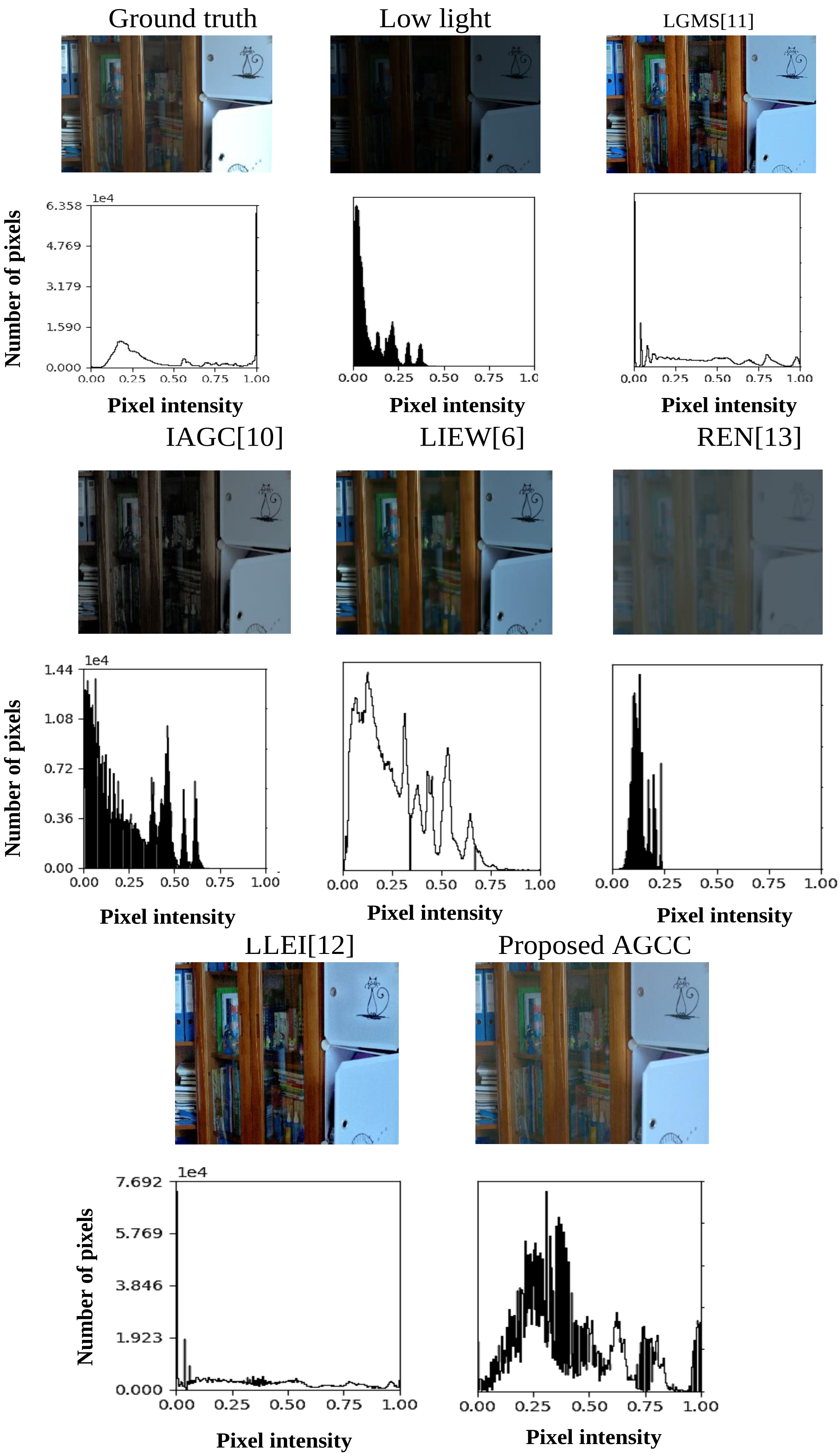

Figure. 5 Compare the result of proposed AGCC and State -of -the -Art Models based on pixel intensity distributed

LGMS[11]) achieve a PSNR value above 0.13. Technically, gamma correction improves the image while maintaining the similarity with the original image. However, these models require further improvement. Fortunately, the model that changes the height to fit the required images has achieved an average BCNR value of up to 18.37. As for Table No. 4, the models based on the style have achieved an SSIM rate of more than sixty per cent with the ground truth, but residual confidence remains. As you can see, the proposed model is correct for you, and the ratio reaches 0.79, which is a very good ratio for retrieving low -light images.

In Fig. 5 noted the pixel intensity distribution of images that restored by the proposed model closely to the normal distribution. Moreover, there is a significant similarity with the pixel intensity of the ground truth. The only distinction between them lies in the pixel intensity in the proposed model, which is related to the color density present. This aspect contributes to the slight error in similarity. Furthermore, compared with other systems, there is a substantial difference in behaviour and in the hyper - density of colors. It indicates that the proposed model effectively mimics the natural distribution of colors and intensity found in the ground truth images, setting it apart from other algorithms in terms of color fidelity and distribution behaviour. The results indicate that the proposed AGCC model offers a substantial improvement in both image quality and similarity to the ground truth, outshining the comparison algorithms. This gives that AGCC has effectively addressed the challenges of image restoration, offering a promising solution for achieving high -quality image enhancement.

Tables 5 and 6 show the results of the proposed model and the compared algorithms on Nan reference datasets regarding NIQE and PRSQUE, respectively.

The proposed model achieved superior results according to the NIQE and BRISQUE metrics, indicating that the features restored and present in the images are of high accuracy. This capability of the proposed system to retrieve images with distinctive qualities can positively impact on performance of machine learning algorithms, the model also restored chromatic properties close to a normal distribution, enhancing the accuracy of the BRISQUE metric. The IAGC model ranked second after the proposed AGCC model due to its closeness to a normal distribution, despite a significant difference between it and the proposed model, and the accuracy of the extracted features. However, the lighting in the other systems tends to be darker rather than light. The closer the pixel density is to unity, the higher the lighting, and the closer the pixel density is to zero, the lower the lighting, as observed in Fig. 5. The proposed algorithm achieved a balanced chromatic density, whereas the other algorithms had chromatic densities leaning towards zero, indicating a tendency towards darkness rather than light.

6.4 Qualitative comparison

When evaluating the quality of images from a visual standpoint, it is essential to focus on several key factors to ensure the image has balanced lighting and high quality. Hence, the image is neither too dark nor overly bright, which helps highlight the image's details and colors without losing details in the shadows or overexposing the light areas. Moreover, the image should have a uniform color balance, where colors appear natural and harmonious. If one of the three channels - red, green, and blue - is significantly higher than the other, the image appears dominant. Additionally, reducing noise in the image without negatively affecting the edges is critical to maintaining image quality. Figs. 6 and 7 show the Qualitative comparison of the proposed AGCC with State -of -the -Art Models.

The images we used to test the proposed algorithm have different illumination intensities, from very low light to medium light and mixed light images, to demonstrate the efficiency of the model in dealing with different conditions. As observed in Figs 6 and 7 the proposed algorithm achieved satisfactory results in reducing noise, achieving color balance, and providing balanced lighting in the image. Furthermore, the proposed algorithm successfully managed to maintain balanced lighting across images with varying lighting conditions, demonstrating its effectiveness in enhancing image quality through improved noise reduction, color balancing, and lighting adjustment. This indicates the superiority of the proposed method in addressing key challenges in image processing, making it a valuable approach for achieving high -quality images.

Through the analysis of the results, both qualitative and quantitative, the proposed AGCC model has demonstrated a significant capability in extracting important features, as evidenced by its accuracy in the NIQE metric. Moreover, It can be considered to have achieved considerable success in retrieving images that are closely similar to the original ones, as shown in the PSNR and the SSIM metrics. Therefore, the proposed model can be considered to have achieved acceptable success in improving low -light images, and it can be considered a successful alternative to current model that work this field.

Received: February 26, 2024. Revised: April 28, 2024.

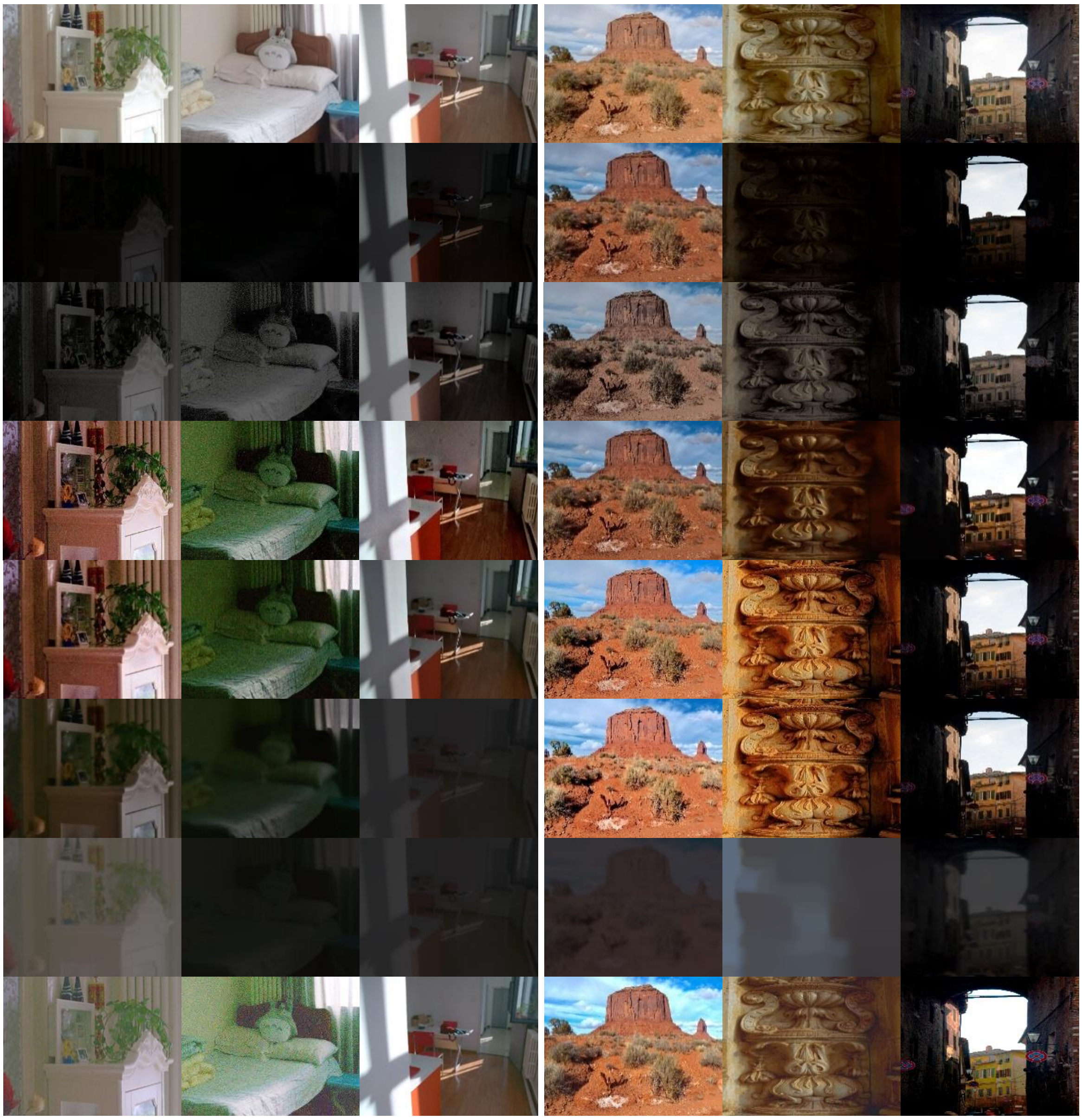

Figure. 6 Compare the result of proposed AGCC and State -of -the -Art models on full reference dataset

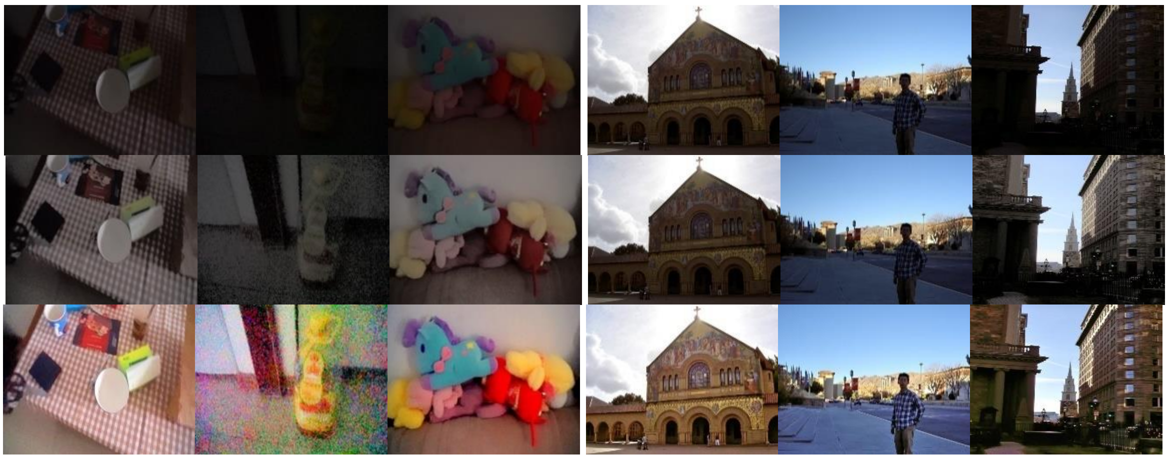

LLEI[12]
LIEW [6]
REN [13]
Proposed AGCC

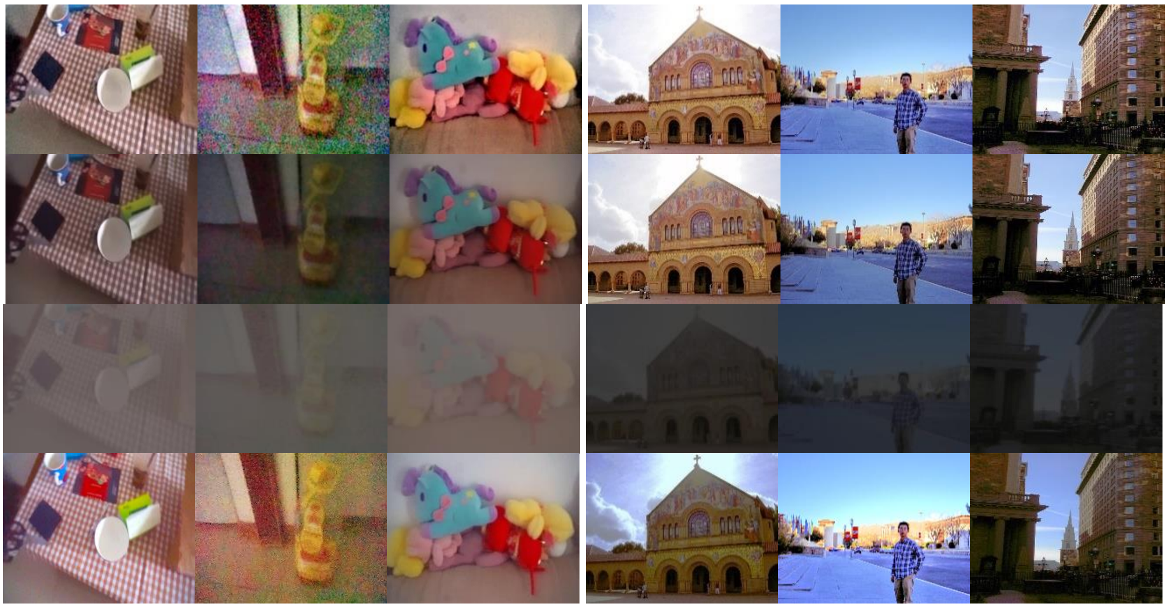

Zero_test Dataset DICM dataset

Low Light
IAGC [10]
LGMS [11]
LLEI[12]
LIEW [6]
REN [13]
Proposed AGCC

VV Dataset LIME dataset

Figure. 7 Compare the result of proposed AGCC and State -of -the -Art models on the nan reference dataset

Received: February 26, 2024. Revised: April 28, 2024.

7. Conclusion

Low -light images inspect basic details such as highlighted edges and color fading. Additionally, the average and standard deviation of the R, G, and B channels are relatively low value. The methods for enhancing low -light images aim to improve the average and standard deviation of the R, G, and B channels. They also maintain a color balance to prevent unwanted new colors in the enhanced image. Some current methods for improving low -light images significantly suffer from issues such as poor lighting, high noise, or undesirable colors (artifacts). Furthermore, these methods face complexity in time and space. In the proposed model, we mitigated these issues by building an adaptive model that adjusts to the lights in the image. The proposed system ensures that the color density distribution of the retrieved images is close to normal distribution. This approach helps maintain the average lighting of the image, ensures the colors are appropriate and prevents veiling as much as possible. The proposed AGCC model achieved a percentage of 0.79 regrades to SSIM and 18.372 on PSNR for the average of the full reference dataset The proposed model achieved the criteria for the importance of features in the restored image, as the BRSQUE rate was 19.05 and NIQE rate of 3.595.

The LIE models generally suffer from restoring images with a very high percentage of darkness. Restoring them leads to a green veil in the final image. The proposed model reduced this tendency but requires additional color balance for the image to be close to the natural images. For future work, the model needs to be integrated with other LIE approaches to increase the accuracy of the resorted images.

Conflicts of Interest

The authors declare no conflict of interest.

Author Contributions

The authors contribution as following: First author Conceptualization; methodology; software, validation. The second author funding acquisition, project administration, and supervision. The third: visualization, writing—review and editing, and writing—original draft preparation.

References

[1] H. Wang, Y. Xu, Z. Wang, Y. Cai, L. Chen, and Y. Li, "Centernet -auto: A multi -object visual detection algorithm for autonomous driving scenes based on improved centernet", *IEEE Transactions on Emerging Topics in Computational Intelligence*, Vol. 7, No. 3, PP.742 -752, 2023.

[2] W. Yin, K. He, D. Xu, Y. Yue, and Y. Luo, "Adaptive low light visual enhancement and high -significant target detection for infrared and visible image fusion", *The Visual Computer*, pp. 1 -20, 2023.

[3] A. S. Alfoudi, A. H. Alsaeedi, M. H. Abed, A. M. Otebolaku, and Y. Sajid Razooqi, "Palm Vein Identification Based on Hybrid Feature Selection Model", *International Journal of Intelligent Engineering and Systems*, Vol. 14, No. 5, pp. 469-478, 2021, doi: 10.22266/ijies2021.1031.41.

[4] J. Hai, Z. Xuan, R. Yang, Y. Hao, F. Zou, F. Lin, and S. Han, "R2rnet: Low -light image enhancement via real -low to real -normal network," *Journal of Visual Communication and Image Representation*, Vol. 90, pp. 103712, 2023.

[5] T. H. Park and I. K. Eom, "Sand -dust image enhancement using successive color balance with coincident chromatic histogram", *IEEE Access*, Vol. 9, pp. 19749 -19760, 2021.

[6] J. J. Jeon, J. Y. Park, and I. K. Eom, "Low -light image enhancement using gamma correction prior in mixed color spaces", *Pattern Recognition*, Vol. 146, pp. 110001, 2024.

[7] X. Feng, J. Li, and Z. Hua, "Low -light image enhancement algorithm based on an atmospheric physical model", *Multimedia Tools and Applications*, Vol. 79, No. 43 -44, pp. 32973 -32997, 2020.

[8] X. Shang, G. Li, Z. Jiang, S. Zhang, N. Ding, and J. Liu, "Holistic Dynamic Frequency Transformer for image fusion and exposure correction", *Information Fusion,* Vol. 102, pp. 102073, 2024.

[9] A. H. Alsaeedi, A. M. Al -juboori, H. H. R. Al - Mahmood, S. M. Hadi, H. J. Mohammed, M. R. Aziz, M. Aljibawi, and R. R. Nuiaa, "Dynamic Clustering Strategies Boosting Deep Learning in Olive Leaf Disease Diagnosis", *Sustainability*, Vol. 15, No. 18, pp. 13723, 2023.

[10] G. Cao, L. Huang, H. Tian, X. Huang, Y. Wang, and R. Zhi, "Contrast enhancement of brightness -distorted images by improved adaptive gamma correction", *Computers & Electrical Engineering*, Vol. 66, pp. 569 -582, 2018.

[11] S. Hao, X. Han, Y. Guo, X. Xu, and M. Wang, "Low -light image enhancement with semi - decoupled decomposition", *IEEE Transactions*

on Multimedia, Vol. 22, No. 12, pp. 3025 -3038, 2020.

[12] J. J. Jeon and I. K. Eom, "Low -light image enhancement using inverted image normalized by atmospheric light", *Signal Processing*, Vol. 196, pp. 108523, 2022.

[13] M. Li, J. Liu, W. Yang, X. Sun, and Z. Guo, "Structure -revealing low -light image enhancement via robust retinex model", *IEEE Transactions on Image Processing*, Vol. 27, No. 6, pp. 2828 -2841, 2018.

[14] J. Tao, J. Wang, P. Zhang, J. Zhang, K. Yung, and W. Ip, "LEGAN: A low -light image enhancement generative adversarial network for industrial internet of smart -cameras", *Internet of Things*, Vol. 25, pp. 101054, 2024.

[15] A. Kumar, R. K. Jha, and N. K. Nishchal, "An improved Gamma correction model for image dehazing in a multi -exposure fusion framework", *Journal of Visual Communication and Image Representation*, Vol. 78, pp. 103122, 2021.

[16] J. Zhou, Q. Gai, D. Zhang, K. -M. Lam, W. Zhang, and X. Fu, "IACC: Cross -Illumination Awareness and Color Correction for Underwater Images Under Mixed Natural and Artificial Lighting", *IEEE Transactions on Geoscience and Remote Sensing*, Vol. 62, pp. 1 -15, 2024.

[17] Y. Du, Q. Sheng, Y. Zhu, J. Li, B. Wang, and X. Ling, "Dehazing Network: Asymmetric Unet Based on Physical Model", *IEEE Transactions on Geoscience and Remote Sensing*, 2024.

[18] T. Rahman, A. Khandakar, Y. Qiblawey, A. Tahir, S. Kiranyaz, S. B. A. Kashem, M. T. Islam, S. Al Maadeed, S. M. Zughaier, and M. S. Khan, "Exploring the effect of image enhancement techniques on COVID -19 detection using chest X -ray images", *Computers in biology and medicine*, Vol. 132, pp. 104319, 2021.

[19] K. W. Houser, T. Esposito, M. P. Royer, and J. Christoffersen, "A method and tool to determine the colorimetric and photobiological properties of light transmitted through glass and other optical materials", *Building and Environment*, Vol. 215, pp. 108957, 2022.

[20] Y. Zhang, X. Guo, J. Ma, W. Liu, and J. Zhang, "Beyond brightening low -light images", *International Journal of Computer Vision*, Vol. 129, pp. 1013 -1037, 2021.

[21] X. Wei, X. Lin, and Y. Li, "DA -DRN: A degradation -aware deep Retinex network for low -light image enhancement", *Digital Signal Processing*, Vol. 144, pp. 104256, 2024.

[22] G. -D. Fan, B. Fan, M. Gan, G. -Y. Chen, and C. P. Chen, "Multiscale low -light image enhancement network with illumination constraint", *IEEE Transactions on Circuits and Systems for Video Technology*, Vol. 32, No. 11, pp. 7403 -7417, 2022.

[23] C. Guo, C. Li, J. Guo, C. C. Loy, J. Hou, S. Kwong, and R. Cong, "Zero -reference deep curve estimation for low -light image enhancement", In: *Proc. of the IEEE/CVF conference on computer vision and pattern recognition*, pp. 1780 -1789, 2020.

[24] A. H. A. Ali Mohsin Al -juboori , Riyadh Rahef Nuiaa, Zaid Abdi Alkareem Alyasseri, Husam Jasim Mohammed, Nor Samsiah Sani, Mohd Isrul Esa, Bashaer Abbuod Musawi, "A Hybrid Cracked Tiers Detection System Based on Adaptive Correlation Features Selection and Deep Belief Neural Networks", *Symmetry*,Vol. 15, No.2, pp.358, 2023.

[25] H. S. Faridul, T. Pouli, C. Chamaret, J. Stauder, E. Reinhard, D. Kuzovkin, and A. Trémeau, "Colour mapping: A review of recent methods, extensions and applications", In: *Proc. of Computer Graphics Forum*, Vol. 35, No. 1, pp. 59 -88, 2016.

[26] N. Huang, Y. Zhang, F. Tang, C. Ma, H. Huang, W. Dong, and C. Xu, "Diffstyler: Controllable dual diffusion for text -driven image stylization", *IEEE Transactions on Neural Networks and Learning Systems*, 2024.

[27] C. Wei, W. Wang, W. Yang, and J. Liu, "Deep retinex decomposition for low -light enhancement. *arXiv* 2018", *arXiv preprint arXiv*, pp. 1808.04560, 1808

[28] W. Wang, C. Wei, W. Yang, and J. Liu, "Gladnet: Low -light enhancement network with global awareness", In: *Proc. of 2018 13th IEEE International Conference on Automatic Face & Gesture Recognition* (FG 2018), pp. 751 -755, 2018.

[29] X. Guo, Y. Li, and H. Ling, "LIME: Low -light image enhancement via illumination map estimation", *IEEE Transactions on Image Processing*, Vol. 26, No. 2, pp. 982 -993, 2016.

[30] C. Lee, C. Lee, and C. -S. Kim, "Contrast enhancement based on layered difference representation", In: *Proc. of 2012 19th IEEE International Conference on Image Processing*, pp. 965 -968, 2012.

[31] V. Vonikakis, Dataset. https://sites.google.com/site/vonikakis/datasets. (Accessed 8 2024)